ISSN: 2229-7359 Vol. 11 No. 25s,2025

https://theaspd.com/index.php

Finite Element Analysis Of Viscous Dissipation On MHD Double Diffusive Free Convective Flow Of An Exponentially Accelerated Inclined Vertical Plate With Ramped Temperature

T.Venkat Laxminarayana¹, Ch Vijaya Bhaskar²

¹Research scholar, School of Engineering, Anurag University, Venkatapur (V), Ghatkesar (M), Telangana, India

³Department of Mathematics, Anurag University, Venkatapur (V), Ghatkesar (M), Hyderabad, Telangana, India

Corresponding Author:

Ch. Vijaya Bhaskar Email: vijay3284@gmail.com

Absract: The current article deals with finite element analysis of viscous dissipation on MHD double diffusive free convective flow of an exponentially accelerated inclined vertical plate with ramped temperature. Initially, flow governing dimensional partial differential equations along with appropriate initial and boundary conditions are converted into non-dimensional form using suitable dimensional quantities and parameters. Later, finite element technique employed to solve the obtained equations, attained results for velocity, temperature, and concentration against various flow parameters discussed and described in detail with the aid of graphs. The influence of specified parameters on Nusselt number, skin friction, & Sherwood number represented in tabular form. Finally in a special case current findings compared with existing literature and a great coordination is identified. The velocity and temperature profiles get accelerated against viscous dissipation. Present numerical investigation can be applied in cancer therapy and oceanography, chemical science, engineering and nuclear industries, food processing, geophysics, movement of biological fluid.

Keywords: Viscous dissipation, MHD, FEM, Porous media, Ramped temperature

1. INTRODUCTION

Natural convection is a type of flow. Here, the movement of fluid happens due to the differences in density caused by temperature changes. There's no outside source like a fan, pump, or anything else doing the work. In free convection, the fluid around it gets heated up. When it happens, it expands and becomes less dense, which means it rises. So, heavier parts go down while lighter parts go up. This creates a movement in the fluid. Now, natural convection can only happen where there's gravity or another force like centrifugal force & Coriolis force. It's really important too! This is because natural convection helps in many ways. For example, it cools high voltage electrical transformers. It also heats homes with electric baseboard heaters and cools down reactor cores in nuclear power plants and electronic devices like chips & transistors. Many studies have taken a closer look at natural convection. Recently, T.Singh et al. [1], escavated about viscous dissipation and radiation absorption effect on MHD free convective heat and mass transfer flow through a highly porous medium with chemical reaction. For instance, Huang et al. [2] studied how MHD (magneto hydrodynamics) affects the flow of non-Newtonian fluids over a vertical permeable plate with heat inside porous media. Agbaje et al. [3] looked into an efficient method for things like Soret & Dufour effects, chemical reactions, and thermal radiation. Then there is Seth et al. [4] who examined how Hall effects impact unsteady MHD natural convection flow of a heat-absorbing fluid past an accelerated moving vertical plate that has ramped temperature. Lastly, Makanda & Gilbert [5] discussed about free convection from a perforated spinning cone that generates heat and has temperaturedependent viscosity along with some partial slip. Nehad Ali et al. [6] found a general solution for MHDfree convection flow over a vertical plate with ramped wall temperature and chemical reactions too! Viscous dissipation is a kind of energy change. It relates kinetic energy from fluid flow to the enthalpy difference across the thermal boundary layer. In simple terms, when a fluid flows, its viscosity steals some motion energy (kinetic energy) and turns it into internal energy. This process causes the fluid to heat up. It's also known as dissipation or viscous dissipation since part of it isn't reversible. A group of researchers,

ISSN: 2229-7359 Vol. 11 No. 25s,2025

https://theaspd.com/index.php

nano fluids behaved in rotating channels while considering entropy generation & viscous dissipation. Then there's Gopal et al. [8] who focused on analyzing higher order chemical reactions on electrically MHD nanofluids while keeping viscous dissipation in mind. Sultana Jahan et al. [9] studied how solar radiation & viscous dissipation affected mixed convective non-isothermal hybrid nanofluid over a moving thin needle. Ahmed and Khidir [10], investigated viscous dissipation along with Ohmic heating & radiation effects on MHD flow past a rotating disk that was situated in a porous medium with changing properties. Zainal et al. [11] studied how viscous dissipation affected MHD hybrid nanofluid flows towards surfaces that stretch or shrink exponentially.

Many other researchers have also looked at numerical or analytical results, usually assuming that conditions at the plate are constant and clear. But many real-life problems need different temperature conditions. Siva Reddy Sheri et al. [12-13] discussed how heat absorption works along with radiative heat transfer when an impulsively moving plate has ramped temperature. Other studies by Suram et al. [14] looked into Soret-dufour effects work within natural convective flow through a porous medium in a rotating system, again with ramped temperatures. Seth et al. [15] studied double diffusive natural convection flow over an inclined plate that accelerated exponentially. Then Vijay Bhaskar et al. [16] examined finite element approximations of MHD flow past a vertical plate embedded in porous media that featured convective boundary conditions & cross diffusion.

The current mathematical investigation explores the effect of heat and mass transfer on natural convection flow past an impulsively moving vertical plate with ramped temperature in the presence of Eckert number. The governing equations are tackled utilizing finite element method. The numerical result is validated by comparing the values of the Nusselt number, Skin friction and Sherwood number obtained through our present scheme with the prior published results.

2. MATHEMATICAL FORMULATION

The physical model and geometrical configeration of the problem is shown in figure 1. We set up a coordinate system. The x'-axis runs along the plate, going upward. The y'-axis is perpendicular to that plate. A magnetic field B_0 applied parallel to the y'-axis. At first, when time $t' \le 0$ starts, the fluid and the plate are both sitting still. T'_{∞} and C'_{∞} . They have a steady temperature and consistent mix of species i.e T'_{∞} and C'_{∞} . Then at time t' > 0, the plate starts to move along the x'-direction, this is against gravity at a speed U(t'). that changes over time. As we go on, during the time frame up to $t' \le t_0$, the temperature and concentration on the surface of the plate go up or down to values of $T'_{\infty} + (T'_{w} - T'_{\infty})t'/t_0$ and $C'_{\infty} + (C'_{w} - C'_{\infty})t'/t_0$. After that, for $t' > t_0$, we keep those temperatures and concentrations steady at T'_{w} and C'_{w} Now here's the interesting fact that, a chemical reaction happening! This reaction is first order, with a constant rate Kr', between the diffusing species and the fluid. The plate, It stretches out infinitely in both the x' & z' directions. Plus, it doesn't conduct electricity. So really, all physical properties, except pressure depend only on y' and t' coordinates.

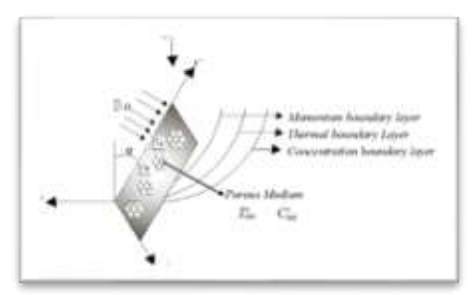


Figure 1. Physical Coordinate Geometry of the Problem

By taking above assumptions into account above, the flow governing equations, under Boussinesq approximation, are given by

$$\frac{\partial u'}{\partial t'} = \upsilon \frac{\partial^2 u'}{\partial v'^2} - \frac{\sigma B_0^2}{\rho} u' - \frac{\upsilon}{K'} u' + g \beta' (T' - T_{\infty}') \cos \alpha + g \beta^* (C' - C_{\infty}') \cos \alpha \tag{1}$$

$$-\frac{1}{\rho}\frac{\partial p}{\partial y} - g\beta'(T' - T'_{\infty})\sin\alpha + g\beta^*(C' - C'_{\infty})\sin\alpha = 0$$
 (2)

ISSN: 2229-7359 Vol. 11 No. 25s,2025

https://theaspd.com/index.php

$$\rho c_{p} \frac{\partial T'}{\partial t'} = k \frac{\partial^{2} T'}{\partial y'^{2}} - \frac{\partial q'_{r}}{\partial y'} - Q_{0} \left(T' - T'_{\infty} \right) + v \rho c_{p} \left(\frac{\partial u'}{\partial y'} \right)^{2}$$

$$\frac{\partial C'}{\partial t'} = D \frac{\partial^{2} C'}{\partial y'^{2}} - K'_{r} \left(C' - C'_{\infty} \right)$$
(4)

Where $u', T', C', g, \beta', \beta^*, v, \sigma, \rho, k, K', c_p, q'_r, Q_0, D$ and K'_r are Fluid velocity: x'-direction is the speed of fluid; Temperature: tells us how hot or cold the fluid is; Species concentration: refers to how much of a certain substance is in the fluid; Acceleration due to gravity: which is pretty much how fast things drop down; Volumetric coefficient of thermal expansion: for species concentration; Kinematic coefficient of viscosity: This one tells us how thick or thin the fluid is; Electrical conductivity: which shows how well the fluid can carry electricity; Fluid density: tells us how heavy or light the fluid is; Thermal conductivity: This means how well heat moves through the fluid; Permeability of a porous medium, Specific heat at constant pressure: tells us how much heat energy a substance needs to change temperature when pressure stays the same; Radiative flux vector: which deals with how energy flows as radiation; Heat absorption coefficient, chemical molecular diffusivity: which explains how substances mix together in our liquid; Chemical reaction parameter: giving us info about reactions happening in that fluid respectively.

Initial and boundary conditions for the problem are specified as

$$u' = 0, T' = T'_{\infty}, C' = C'_{\infty} \text{ for } y' \ge 0 \text{ and } t' \le 0$$

$$u' = U_{0} \exp(a't') \text{ at } y' = 0 \text{ for } t' > 0$$

$$T' = T'_{\infty} + \left(T'_{w} - T'_{\infty}\right)t'/t_{0}, C' = C'_{\infty} + \left(C'_{w} - C'_{\infty}\right)t'/t_{0} \text{ at } y' = 0 \text{ for } 0 < t' \le t_{0}$$

$$T' = T'_{w}, C' = C'_{w} \text{ at } y' = 0 \text{ for } t' > t_{0}$$

$$u' \to 0, T' \to T'_{w}, C' \to C'_{w} \text{ as } y' \to \infty \text{ for } t' > 0$$

$$(5)$$

For a fluid that's really thick, Azzam [17] noted that besides emitting light, there's also self-absorption going on. This means it kind of absorbs what it gives off. It's usually the case that the absorption coefficient changes with wavelength and can be quite substantial like Bestman [18] said. So, we can use something called Rosseland approximation when looking at the radiative flux vector q'_r . Thus

$$q'_{r} = -\frac{4\sigma^{*}}{3k^{*}} \frac{\partial T^{'}}{\partial y'} \tag{6}$$

Where k^* is mean absorption co-efficient and σ^* is Stefan-Boltzmann constant and neglecting the higher order terms ($T'-T'_{\infty}$), we obtain

$$T^{'4} \approx 4T_{\infty}^{'3} T' - 3T_{\infty}^{'4}$$
 (7)

Making use of Equations (6) and (7) in Equation (3), we Obtain

$$\frac{\partial T'}{\partial t'} = \frac{k}{\rho c_p} \frac{\partial^2 T'}{\partial y'^2} + \frac{1}{\rho c_p} \frac{16\sigma^* T_{\infty}^{3}}{3k^*} \frac{\partial T'^2}{\partial y'^2} - \frac{Q_0}{\rho c_p} (T' - T_{\infty}') + \nu \left(\frac{\partial u'}{\partial y'}\right)^2$$
(8)

following similarity parameters

$$y = \frac{y'}{U_{0}t_{0}}, \quad u = \frac{u'}{U_{0}}, \quad t = \frac{t'}{t_{0}}, T = \frac{(T' - T_{\infty}')}{(T_{w}' - T_{\infty}')}, C = \frac{(C' - C_{\infty}')}{(C_{w}' - C_{\infty}')}, M = \frac{\sigma B_{0}^{2} v}{\rho U_{0}^{2}},$$

$$K = \frac{K' U_{0}^{2}}{v^{2}}, Gr = \frac{g\beta' v(T_{w}' - T_{\infty}')}{U_{0}^{3}}, Gc = \frac{g\beta * v(C_{w}' - C_{\infty}')}{U_{0}^{3}}, Pr = \frac{v\rho c_{p}}{k},$$

$$N = \frac{16\sigma^{*} T_{\infty}^{3}}{3kk^{*}}, \phi = \frac{vQ_{0}}{\rho c_{p} U_{0}^{2}}, Ec = \frac{U_{0}^{2}}{c_{p} (T_{w}' - T_{\infty}')}, Kr = \frac{vKr'}{U_{0}^{2}}, Sc = \frac{v}{D}$$

$$(9)$$

In view of equations (9), equations (8) and (4) reduce to the following $\frac{\partial u}{\partial t} = \frac{\partial^2 u}{\partial v^2} + GrT \cos\theta + Gc C \cos\theta - \left(M + \frac{1}{K}\right)u \tag{10}$

$$\frac{\partial T}{\partial t} = \frac{(N+1)}{\Pr} \frac{\partial^2 T}{\partial v^2} - \phi T + Ec \left(\frac{\partial u}{\partial v}\right)^2 \tag{11}$$

ISSN: 2229-7359 Vol. 11 No. 25s,2025

https://theaspd.com/index.php

$$\frac{\partial C}{\partial t} = \frac{1}{Sc} \frac{\partial^2 C}{\partial y^2} - KrC \tag{12}$$

According to the above non-dimensional process the characteristic time t_0 can be defined as

$$t_0 = \frac{v}{{U_0}^2}$$

Using (8) the initial boundary conditions (4), in non-dimensional form reduces to

$$u = 0, \quad T = 0, C = 0 \quad \text{for} \quad y \ge 0 \quad \text{and} \quad t \le 0$$

$$u = \exp(bt) \quad \text{at} \quad y = 0 \quad \text{for} \quad t > 0,$$

$$T = t, C = t \quad \text{at} \quad y = 0 \quad \text{for} \quad 0 < t \le 1,$$

$$T = 1, C = 1 \quad \text{at} \quad y = 0 \quad \text{for} \quad t > 1,$$

$$u \to 0, \quad T \to 0, C \to 0 \quad \text{as} \quad y \to \infty \quad \text{for} \quad t > 0$$
(13)

3. METHOD OF SOLUTION

The non-linear dimensionless PDEs (10) - (12) along with initial and boundary conditions (13) are solved numerically using the finite element method. It's actually simple and effective. This method consists of following five fundamental steps: discretization of the domain, derivation of element equations, assembly of element equations, imposition of boundary conditions and solution of the system of equations. An excellent description of these steps presented in the text books Reddy [19], Bathe [20]. By using this procedure, the whole domain is divided in to a set of 80 intervals of equal length, 0.1. At each node 3 functions are to be evaluated; hence after assembly of the elements, we obtain a set of 243 equations. The system of equations after assembly of the elements, are nonlinear and consequently an iterative scheme is employed to solve the matrix system, which is solved by using the Gauss Seidel method. This process is repeated until the desired accuracy of 10⁶ is obtained. Hence, the finite element method is stable and convergent.

Skin-friction coefficient at the plate:
$$\tau = \left[\frac{\partial u}{\partial y}\right]_{y=0}$$
 (14)

Then there's the rate of heat transfer coefficient at the plate:
$$Nu = -\left[\frac{\partial T}{\partial y}\right]_{y=0}$$
 (15).

The rate of mass transfer coefficient at the plate
$$Sh = -\left[\frac{\partial C}{\partial y}\right]_{y=0}$$
 (16)

4. VALIDATION OF NUMERICAL METHOD

To validate the numerical method employed for the solution of the present problem under some assumptions (in the absence of Eckert number) was compared with the problem of MHD double diffusive natural convection flow over exponentially accelerated inclined plate by Seth et al. (2017) and are displayed in tables 1-3. These comparisons show good agreement between the results up to four decimal places..

Now, the Table 1 shows how skin friction changes with different values of Gr, Gc, ϕ, N, b and t. What we found is interesting. For plates with ramped temperature & concentration, as well as for isothermal plates with uniform surface concentration, skin friction goes up with higher values of ϕ and t. But there's a reversal observation as Skin friction actually goes down when Gr, Gc, N and b increase.

Table 2, it reveals how the Nusselt number varies with ϕ , N and t. The Nusselt number speeds up when ϕ increases but slows down as N rises this is true for both isothermal plates and ramped temperature plates. Also worth noting: for ramped temperatures, Nu increases with t; however, there's a reverse trend for isothermal plates.

Table 3. It highlights how the Sherwood number changes with different values of *Kr*, *t* and *Sc* for both ramped and uniform surface concentrations. It's clear that the Sherwood number goes up when both *Kr* and *Sc* increase this holds true for both types of surface concentrations. However! For ramped surface concentration, it climbs over time; but if we talk about uniform surface concentration, that one actually

ISSN: 2229-7359 Vol. 11 No. 25s,2025

https://theaspd.com/index.php

sees its Sherwood number drop as time goes on. These comparisons and observations give us a deeper insight into the problem which we're exploring in this paper.

Table 1. Comparison of Skin friction for Ramped temperature plate with ramped surface concentration

and Isothermal plate with uniform surface concentration

nd Isothermai piate with uniform surface concentration									
						Results by Seth et al. (2017)		Current Results	
						Ramped	Isothermal	Ramped	Isothermal
		4		1		temperature	plate	temperature	plate uniform
Gr	Gc	ϕ	N	b	t	plate ramped	uniform	plate ramped	surface
						surface	surface	surface	concentration
						concentration	concentratio	concentratio	
							n	n	
2	5	3	3	0.2	0.	2.4246 1.6457		2.42459	1.64570
6	5	3	3	0.2	0.	2.1115	0.5175	2.11150	0.51750
10	5	3	3	0.2	0. 5	1.7983	0.2315	1.79830	0.23149
10	3	3	3	0.2	Ö.	1.9531	0.5266	1.95310	0.52659
10	5	3	3	0.2	0.	1.7983	0.4175	1.79829	0.41749
10	7	3	3	0.2	0.	1.6436	0.2315	1.64359	0.23149
10	5	3	3	0.2	0.	1.8725	0.3496	1.87250	0.34959
10	5	5	3	0.2	0.	1.9025	0.4524	1.90250	0.45240
10	5	7	3	0.2	0.	1.9280	0.5342	1.92800	0.53420
10	5	3	1	0.2	0.	1.9531	0.5266	1.95309	0.52660
10	5	3	3	0.2	0.	1.8725	0.3496	1.87250	0.34959
10	5	3	5	0.2	0.	1.8312	0.2603	1.83120	0.26029
10	5	3	3	0.2	0.	2.3315	0.5801	2.33149	0.58010
10	5	3	3	0.8	0.	3.0317	1.2802	3.03167	1.28020
10	5	3	3	1.4	0.	3.8915	2.1400	3.89149	2.14000
10	5	3	3	0.2	0.	2.3315	0.5801	2.33150	0.58010
10	5	3	3	0.2	0.	2.4531	0.5866	2.45310	0.58660
10	5	3	3	0.2	0.	2.5737	0.5918	2.57369	0.59179

Table 2. Comparison of Nusselt number for Ramped temperature and Isothermal plate

ϕ	t	N	Results by Seth et al. (2017)		Current Results	
			Ramped	Isothermal	Ramped	Isothermal
			temperature	plate	temperature	plate
3	0.5	1	0.6837	1.0521	0.68369	1.05210
3	0.5	3	0.4834	0.7439	0.48339	0.74389
3	0.5	5	0.3947	0.6074	0.39470	0.60739
3	0.3	3	0.4699	1.0961	0.46989	1.09610
3	0.5	3	0.6837	1.0521	0.68369	1.05210
3	0.7	3	0.8926	1.0394	0.89259	1.03940
3	0.5	3	0.6837	1.0521	0.68370	1.05210
5	0.5	3	0.7986	1.3375	0.79859	1.33749
7	0.5	3	0.9006	1.5778	0.90060	1.57779

Table3. Comparison of Sherwood number for Ramped and uniform surface concentration

Kr	t	Sc		
IX/		SC	Results by Seth et al. (2017)	Current Results

ISSN: 2229-7359 Vol. 11 No. 25s,2025

https://theaspd.com/index.php

			Ramped surface Concentration	Uniform Surface Concentration	Ramped surface Concentration	Uniform Surface Concentration
	2.5	2.22	2.5022	2.0202		
3	0.5	0.22	0.5800	0.8282	0.58000	0.82820
3	0.5	0.32	0.6995	0.9989	0.69949	0.99890
3	0.5	0.60	0.9578	1.3678	0.95779	1.36779
3	0.3	0.22	0.5074	0.8628	0.50739	0.86279
3	0.5	0.22	0.5800	0.8283	0.58000	0.82830
3	0.7	0.22	0.7143	0.8183	0.71429	0.81830
1	0.5	0.22	0.5472	0.5472	0.54719	0.54719
3	0.5	0.22	0.5800	0.8283	0.58000	0.82829
5	0.5	0.22	0.6440	1.0531	0.64400	1.05310

5. RESULTS AND DISCUSSION

The developed MATLAB code can be used with a great confidence in the numerical results presented subsequently to study the problem and the results are as follows

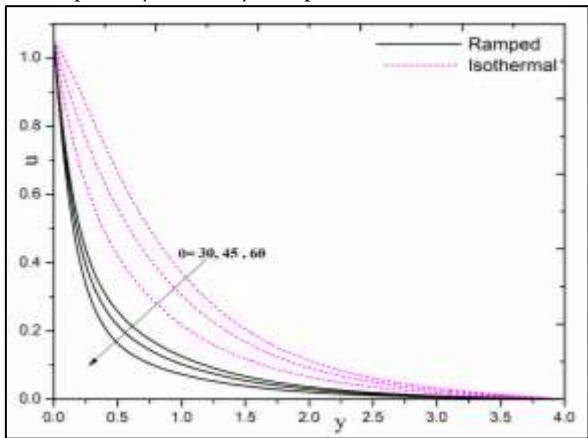


Figure 2. Influence of θ on Velocity

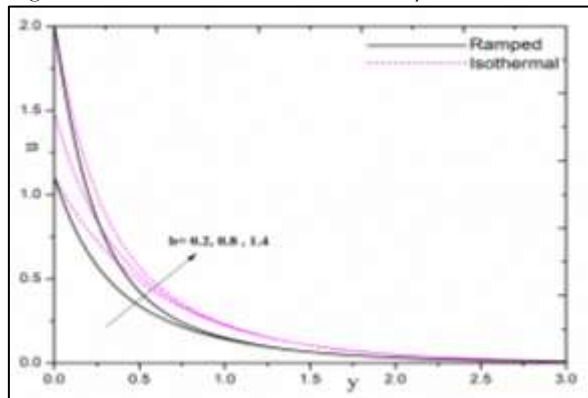


Figure 3. Influence of *b* on Velocity

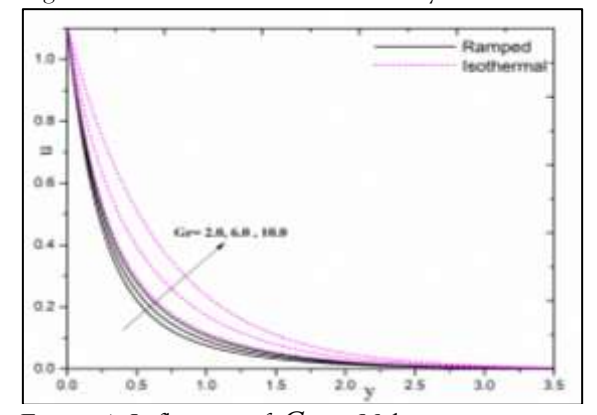


Figure 4. Influence of Gr on Velocity

International Journal of Environmental Sciences ISSN: 2229-7359 Vol. 11 No. 25s,2025

https://theaspd.com/index.php

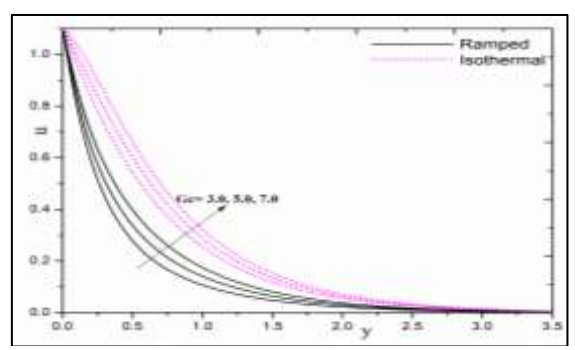


Figure 5. Influence of Gc on Velocity

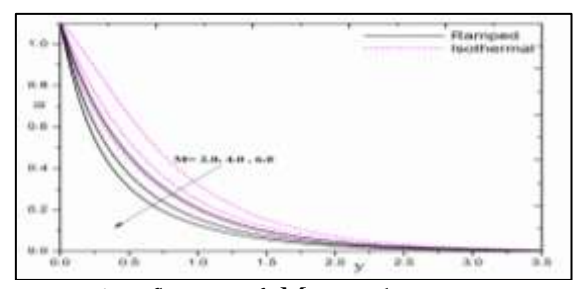


Figure 6. Influence of M on Velocity

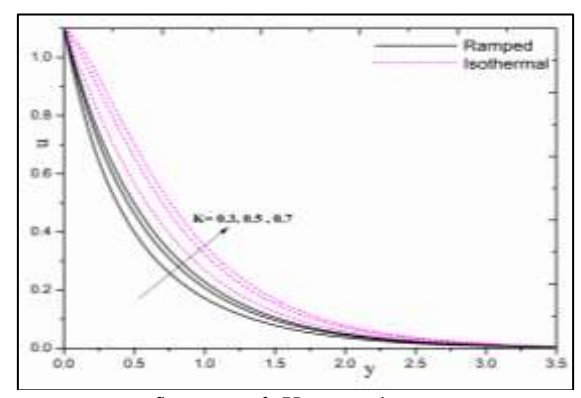


Figure 7. Influence of *K* on Velocity

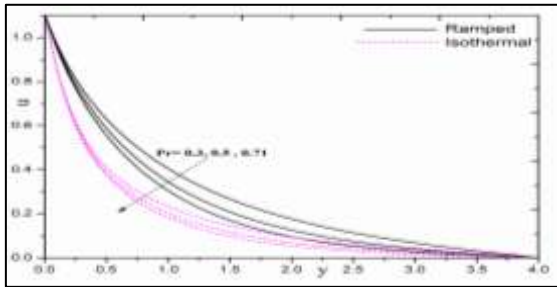


Figure 8(a). Influence of Pr on Velocity

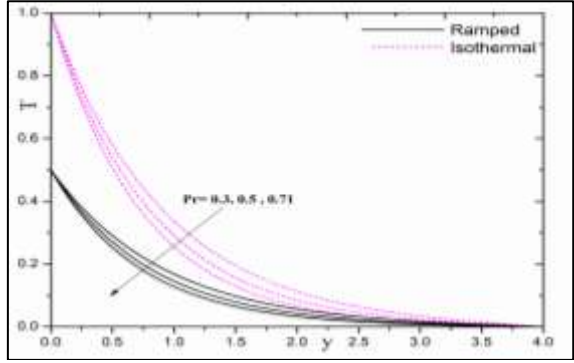


Figure 8(b). Influence of Pr on temperature

International Journal of Environmental Sciences ISSN: 2229-7359 Vol. 11 No. 25s,2025

https://theaspd.com/index.php

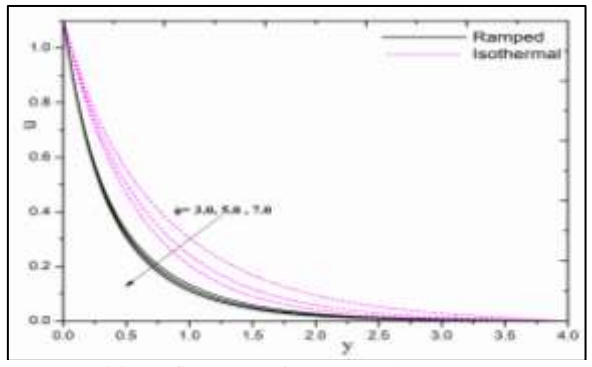


Figure 9(a). Influence of ϕ on Velocity

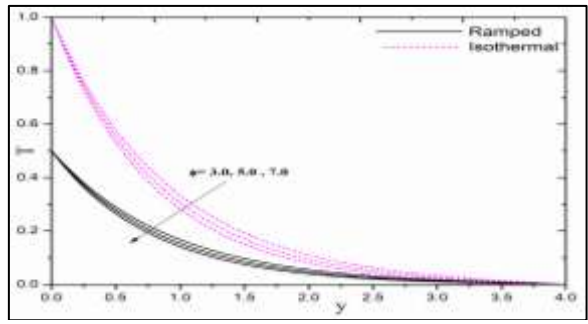


Figure 9(b). Influence of ϕ on Temperature

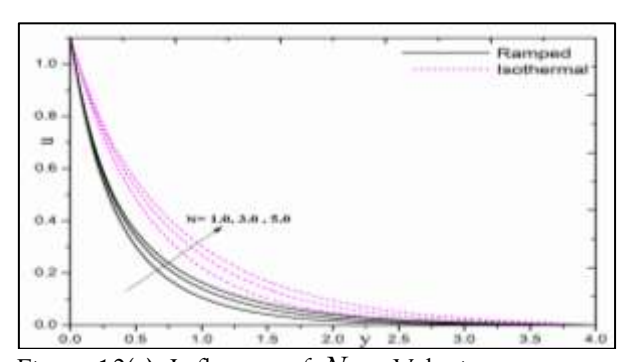


Figure 10(a). Influence of \overline{N} on Velocity

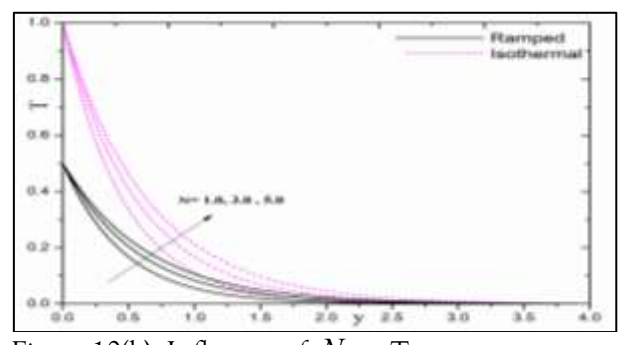


Figure 10(b). Influence of N on Temperature

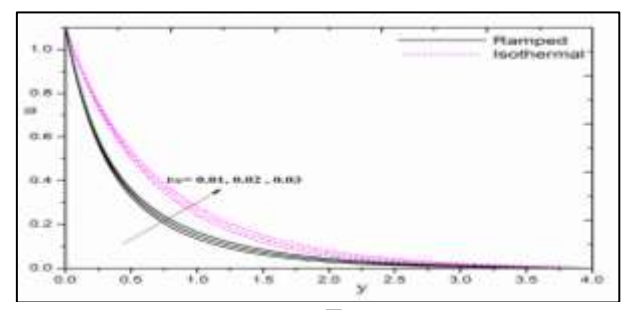


Figure 11(a). Influence of Ec on Velocity

ISSN: 2229-7359 Vol. 11 No. 25s,2025

https://theaspd.com/index.php

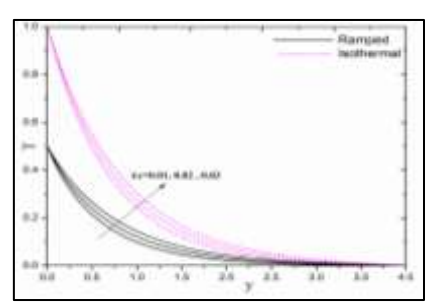


Figure 11(b). Influence of Ec on Temperature

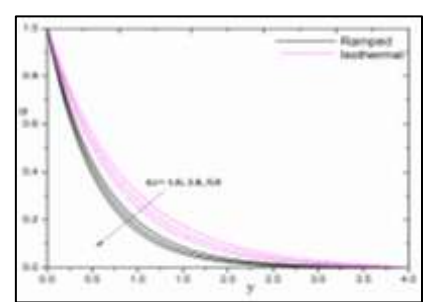


Figure 12(a). Influence of *Kr* on Velocity

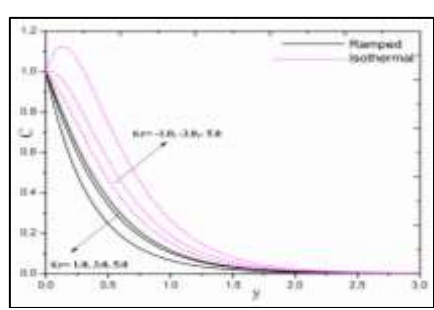


Figure 12(b). Influence of Kr on Concentration

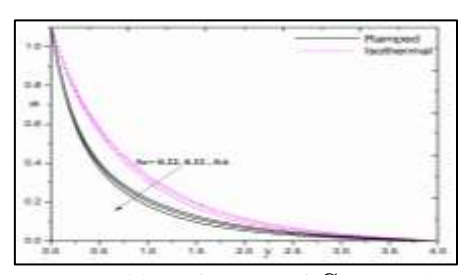


Figure 13(a). Influence of Sc on Velocity Profile

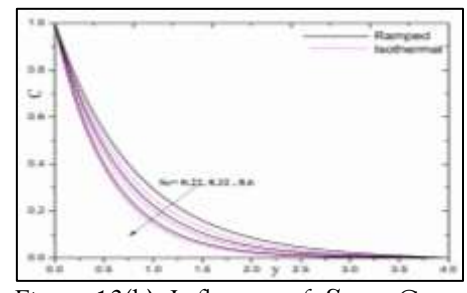


Figure 13(b). Influence of Sc on Concentration

To investigate the effects of various parameters on flow-field in the boundary layer region, numerical values of fluid velocity, temperature and concentration are computed from the numerical solutions, are depicted graphically in Figures. 2–13(b) for various values of angle of inclination, accelerating parameter, thermal Grashof number, solutal Grashof number, magnetic parameter, permeability parameter, Prandtl number, thermal heat absorption coefficient, radiation parameter, Eckert number, chemical reaction

ISSN: 2229-7359 Vol. 11 No. 25s,2025

https://theaspd.com/index.php

parameter and Schmidt number .In the present study we adopted the following parameter values of finite element computations.

$$Gr = 1.0, Gc = 1.0, M = 2.0, K = 0.2, Pr = 0.71, R = 1.0, Q = 1.0, Ec = 0.01, Sc = 2.0, Kr = 2.0, t = 0.5$$

Figure 2 displays the velocity profile for different values of angle of inclination for both ramped temperature and isothermal plates. From this Figure it is identified that velocity \boldsymbol{u} gets reduced on increasing the values of angle of inclination $\boldsymbol{\theta}$. As $\boldsymbol{\theta}$ Increases the effect of the buoyancy force decreases since it is multiplied by $\cos \, \boldsymbol{\theta}$, so the velocity profile decreases. Figure 3 shows the influence of acceleration parameter \boldsymbol{b} on velocity \boldsymbol{u} . It is noticed that the region near to the plate get speed up with the increasing values of acceleration parameter and gradually the influence of \boldsymbol{b} becomes negligible in the region far from the plate. This conveys that higher the fluid motion gets fast near to the moving plate due to higher plate velocity

Figure 4 displays the behavior of velocity profiles for various values of thermal Grashof number for both ramped temperature and isothermal plates. Since thermal Grashof number Gr is the ratio of the thermal buoyancy force and viscous hydrodynamic force. From figure 4 it is observed that velocity profile increases with the increasing of Gr in the boundary layer region. This is due the reason that the thermal buoyancy force tends to accelerate fluid flow. Figure 5 depicts velocity profiles for various values of solutal Grashoff number for both ramped temperature and isothermal plates. Solutal Grashoff number is the ratio of the buoyancy force and viscous hydrodynamic force. From Figure 5 it is noticed that velocity profile increases with the increasing of Solutal Grashof number Gc in boundary layer region. This due to the reason that concentration buoyancy force has a tendency to accelerate fluid velocity for both ramped temperature and isothermal plate.

Figure 6 conveys velocity profiles for various values of magnetic field for both ramped temperature and isothermal plate. From Figure. 6 it is clear that the velocity profile begins to decrease with increasing of M. The presence of magnetic field normal to the flow in an electrically conducting fluid introduces a Lorentz force which acts against the flow. This resistive force tends to slow down the flow and hence the fluid velocity decreases with increasing the magnetic field parameter. Figure 7 explains velocity profiles for various values of permeability parameter for both ramped temperature and isothermal plate. From figure. 7 it is conformed that velocity profile increases with the increase in permeability parameter K. This is expected since when the holes of porous medium become larger, the resistive of the medium may be neglected. This implies that the resistance in porous medium which tends to accelerate flow of the fluid for both ramped and isothermal plates.

Figures 8(a) and 8(b) display the velocity and temperature profiles for different values of Prandtl number for both ramped and isothermal plates. Prandtl number is the ratio of momentum diffusivity (kinematic viscosity) to thermal diffusivity. It can be related to the thickness of the thermal and velocity boundary layers. It is actually the ratio of velocity boundary layer to thermal boundary layer. Figure 8(a) reveals that velocity profile decreases with the increasing of Pr. This implies that thermal diffusion tends to accelerate fluid velocity throughout boundary layer region. This happens due to the fact that thermal diffusion provides an impetus to the thermal buoyancy force. Figure 8(b) explains that temperature profile decreases with the increasing of Pr. Since Pr signifies the relative effects of viscosity to thermal conductivity. This implies that, thermal diffusion tends to enhance fluid temperature. Figures 9(a) and 9(b) demonstrate the velocity and temperature profiles for several values of heat absorption for both ramped temperature and isothermal plates. From 9(a) and 9(b) it is clear that fluid velocity and temperature profiles decrease with increasing of ϕ . This is due to the reason that, heat absorption tends to retard fluid velocity and temperature throughout boundary layer region. This may be attributed to the fact that the tendency of heat absorption (thermal sink) is to reduce the fluid temperature which causes the strength of thermal buoyancy force to decrease resulting in a net reduction in the fluid velocity

Figures 10(a) and 10(b) depict velocity and temperature profiles for several values of radiation parameter for both ramped temperature and isothermal plate. From these two Figures it is observed that fluid velocity and temperature increase with the increasing of radiation parameter in the boundary layer region which implies that thermal radiation tends to enhance fluid velocity and temperature for both ramped temperature and isothermal plates. Figures 11(a) and 11(b) describe velocity and temperature profiles for several values of Eckert number on for both ramped and isothermal plate. The Eckert number is the relationship between kinetic energy in the flow and the enthalpy. It represents the change of kinetic energy into internal energy by work done against the viscous fluid stresses. From 11(a) and 11(b) it is clear

ISSN: 2229-7359 Vol. 11 No. 25s,2025

https://theaspd.com/index.php

that there is an increase in fluid velocity and temperature due to the fact that greater viscous dissipative heat causes a rise in the velocity as well as the temperature.

Figures 12(a) and 12(b) portray velocity and concentration profiles for different values of chemical reaction for both ramped and isothermal plates. From 12(a) and 12(b) it is observed that an increase in chemical reaction parameter leads to a decrease in both the values of velocity and concentration. This is due to fact that distinct velocity acceleration occurs near the wall after which profiles decay smoothly to the stationary value in free stream. Chemical reaction therefore boosts momentum transfer, i.e., accelerates the flow. Figures 13(a) and 13(b) give the details about the profiles of velocity and concentration for various values of Schmidt number for both ramped temperature and isothermal plates. From 13(a) and 13(b) it is noticed that both velocity and concentration distribution diminish at all points of the flow field with the increase of the Schmidt number. This confirms that the heavier diffusing species have a greater retarding influence on velocity and concentration distribution of the flow field in case of both ramped temperature and isothermal plates.

6. CONCLUSIONS

The present numerical analysis deals with the effect of viscous dissipation on natural convection flow past an impulsively moving vertical plate with ramped temperature. The numerical solutions of momentum, energy and concentration equations are obtained by Finite element method. Graphical results of velocity, temperature and concentration against different flow parameters are obtained by MATLAB. Effect of Skin friction, Nusselt number and Sherwood number on flow field is presented in a tabular form and at the same time they are compared with the earlier results presented by Seth et al. (2017). The overall conclusions for both ramped and isothermal plates are: the velocity increases with the increase of thermal buoyancy force Gr concentration buoyancy force Gc, permiability parameter K Ecert number Ec and it has reverse tendency with the increase of magnetic parameter M, Prandtl number Fr, heat absorption ϕ radiation parameter Fr0 N Chemical reaction parameter Fr1 N Concentration decreases with the increase of Prandtl number Fr2, heat absorption Fr3 and radiation parameter Fr4 N Concentration decreases with the increase of Chemical reaction parameter Fr3 N Concentration decreases with the increase of Chemical reaction parameter Fr3 N Concentration decreases with the increase of Chemical reaction parameter Fr3 N Concentration decreases with the increase of Chemical reaction parameter Fr4 N Concentration decreases with the increase of Chemical reaction parameter Fr4 N Concentration decreases with the increase of Chemical reaction parameter Fr4 N Concentration decreases with the increase of Chemical reaction parameter Fr4 N Concentration decreases with the increase of Chemical reaction parameter Fr5 N Concentration decreases with the increase of Chemical reaction parameter Fr5 N Concentration decreases with the increase of Chemical reaction parameter Fr6 N Concentration decreases with the increase of Chemical reaction parameter Fr6 N Concentration decreases with the i

REFERENCES

- [1] T. Singh and H. Pal, "Viscous dissipation and radiation absorption effect on MHD free convective heat and mass transfer flow through a highly porous medium with chemical reaction," strpm, vol. 16, no. 3, 2025.
- [2] C.-J. Huang, H.-P. Hsu, and H. Ay, "Influence of MHD on free convection of non-Newtonian fluids over a vertical permeable plate in porous media with internal heat generation," *Frontiers in Heat and Mass Transfer (FHMT)*, vol. 13, 2019.
- [3] A. Leach and P. Sibanda, "Efficient large spectral collocation method for MHD laminar natural convection flow from a vertical permeable flat plate with uniform surface temperature, Soret, Dufour, chemical reaction and thermal radiation," *IAENG* International Journal of Applied Mathematics, vol. 50, no. 3, pp. 1–15, 2020.
- [4] G. Seth, "Hall effects on unsteady MHD natural convection flow of a heat absorbing fluid past an accelerated moving vertical plate with ramped temperature," *Emirates Journal of Engineering Research*, vol. 19, pp. 19–32, 2014.
- [5] G. Makanda, "Free Convection from a Perforated Spinning Cone with Heat Generation, Temperature-Dependent Viscosity and Partial Slip," *Advanced Science Letters*, vol. 24, pp. 8271–8275, 2018, doi: 10.1166/asl.2018.12539.
- [6] N. A. Shah, A. A. Zafar, and S. Akhtar, "General solution for MHD-free convection flow over a vertical plate with ramped wall temperature and chemical reaction," *Arab. J. Math.*, vol. 7, pp. 49–60, 2018, doi: 10.1007/s40065-017-0187-z.
- [7] A. Dawar, Z. Shah, W. Khan, M. Idrees, and S. Islam, "Unsteady squeezing flow of magnetohydrodynamic carbon nanotube nanofluid in rotating channels with entropy generation and viscous dissipation," *Advances in Mechanical Engineering*, vol. 11, 2019, Art. no. 1687814018823100, doi: 10.1177/1687814018823100.
- [8] D. Gopal et al., "Numerical analysis of higher order chemical reaction on electrically MHD nanofluid under influence of viscous dissipation," *Alexandria Engineering Journal*, vol. 60, pp. 1861–1871, 2021, doi: 10.1016/j.aej.2020.11.034.
- [9] S. Jahan, M. Ferdows, M. D. Shamshuddin, and K. Zaimi, "Effects of Solar Radiation and Viscous Dissipation on Mixed Convective Non-Isothermal Hybrid Nanofluid over Moving Thin Needle," *Journal of Advanced Research in Micro and Nano Engineering*, vol. 3, pp. 1–11, 2021.
- [10] A. A. Khidir, "Viscous dissipation, Ohmic heating and radiation effects on MHD flow past a rotating disk embedded in a porous medium with variable properties," *Arab. J. Math.*, vol. 2, pp. 263–277, 2013, doi: 10.1007/s40065-013-0072-3.
- [11] N. A. Zainal, R. Nazar, K. Naganthran, and I. Pop, "Viscous dissipation and MHD hybrid nanofluid flow towards an exponentially stretching/shrinking surface," *Neural Comput & Applic.*, vol. 33, pp. 11285–11295, 2021, doi:10.1007/s00521-020-05645-5.
- [12] S. R. Sheri, R. S. Raju, and S. A. Kumar, "Transient Approach to Heat Absorption and Radiative Heat Transfer Past an Impulsively Moving Plate with Ramped Temperature," *Procedia Engineering*, vol. 127, pp. 893–900, 2015, doi: 10.1016/j.proeng.2015.11.427.

ISSN: 2229-7359 Vol. 11 No. 25s,2025

https://theaspd.com/index.php

[13] S. R. Sheri and A. K. Suram, "Finite Element Analysis of Heat and Mass Transfer past an Impulsively Moving Vertical Plate with Ramped Temperature," *J. Appl. Sci. Eng.*, vol. 19, pp. 385–392, 2016, doi: 10.6180/jase.2016.19.4.01.

[14] S. R. Sheri, J. Ali, and A. K. Suram, "Thermal-diffusion and diffusion-thermo effects on MHD natural convective flow through porous medium in a rotating system with ramped temperature," *International Journal of Numerical Methods for Heat & Fluid Flow*, vol. 27, pp. 2451–2480, 2017, doi: 10.1108/HFF-09-2016-0349.

[15] G. Seth, R. Tripathi, R. Sharma, and A. Chamkha, "MHD Double Diffusive Natural Convection Flow Over Exponentially Accelerated Inclined Plate," *Journal of Mechanics*, vol. 33, pp. 87–99, 2017, doi: 10.1017/jmech.2016.56.

[16] Ch. V. Bhaskar, S. R. Sheri, and A. K. Suram, "Finite element approximation of MHD flow past a vertical plate in an embedded porous medium with a convective boundary condition and cross diffusion," in *Proc. Int. Conf. Mathematical Sciences and Applications (ICMSA-2019)*, Hyderabad, India, 2020.

[17] G. E.-D. A. Azzam, "Radiation Effects on the MHD Mixed Free-Forced Convective Flow Past a Semi-Infinite Moving Vertical Plate for High Temperature Differences," *Phys. Scr.*, vol. 66, p. 71, 2002, doi: 10.1238/Physica.Regular.066a00071.

[18] K. J. Bathe, Finite Element Procedures. New Jersey: Prentice-Hall, 1996.

[19] A. R. Bestman, "Title unknown," Int. J. Numer. Methods Eng., vol. 21, pp. 899-908, 1985.